Dust induced structure formation

Peter Woitke

Institut für Astronomie und Astrophysik
Technische Universität Berlin, Hardenbergstr. 36, 10623 Berlin, Germany
woitke@physik.tu-berlin.de

Abstract

Astrophysical systems in which the phase transition between gas and solid state occurs (dust forming systems) are characterized by a complex interplay between the various physical interactions. Among them are the hydrodynamic and thermodynamic processes of the dust-gas mixture, the chemical processes of the phase transition and the radiative transfer. Due to the additional feedbacks introduced by the dust formation, the system may host various dynamical, thermal or radiative instabilities. In this paper, we identify such instabilities and examine the question whether they can trigger self-organization processes (e. g. cloud formation) revealed by recent high angular resolution observations of dusty objects.

Beside a dynamical instability found in spherically symmetric, time-dependent models of circumstellar dust shells around AGB stars (dust induced shock waves) we report on thermal bifurcations in the outer atmospheres of R Coronae Borealis stars, and put special emphasis on a radiative instability which occurs when combining time-dependent models for the dust formation process with multi-dimensional radiative transfer. It is demonstrated that due to this instability, the dust formation in C-star environments may provoke a self-organization of matter, leading to radially aligned dust structures, because the formation of dust is facilitated behind already condensed zones which cast a shadow into the circumstellar envelope, thereby improving the conditions for subsequent dust formation.

1 Introduction

Recent technical improvements in observational instruments, detectors, platforms, and methods (e. g. speckle interferometry) have enabled mankind to look at the objects in space with an angular resolution of only a few milliarcseconds. Thereby, convincing evidence has been accumulated in the last years that the mainly gaseous matter in astrophysical objects is usually not smooth and homogeneous, but often reveals an internal structure in form of a clumpy, patchy or cloudy distribution in space on different length scales. These observations strongly suggest that structure formation and self-organization processes are common in astrophysical media. In particular, dispersivity and inhomogeneities are observed in those objects, where dust formation takes place or has taken place in the past, e. g. the circumstellar envelopes of AGB and post-AGB stars, planetary nebulae, nova and supernovae explosions, and the hot environments of R Coronae Borealis and Wolf Rayet stars. Some of these observations are outlined in Sect. 2.

The cause of the spatio-temporal structure formation is usually ascribed to certain instabilities inherent in the considered physical system which amplify initial perturbations arising e. g. from fluctuations. Especially well-known in astrophysics is the large family of dynamical instabilities, where disturbances of the velocity field play a crucial role (e. g. turbulence, gravitational and convective instabilities, Rayleigh-Taylor, Richtmyer-Meshkov, Kelvin-Helmholtz, see e. g. review by Inogamov 1999). There are, however, also thermal instabilities which are related to the energy balance of the gas as affected by chemical processing like phase transitions, for example the multi-phase stability of the interstellar medium (Biermann et al. 1972) or the so-called "thermal bifurcations" in the outer atmospheres of stars (in particular the sun, Ayres 1981, Muchmore 1986, Cuntz & Muchmore 1994). Furthermore, radiative instabilities may be induced e. g. by a temperature-dependent opacity and its non-local feedback on the radiation field and hence on the temperature structure of the medium, which are often closely related to the thermal instabilities (e. g. Spiegel 1957, Trujillo Bueno & Kneer 1990, McDonald & Mullan 1997).

This paper investigates instabilities and related structure formation processes in dust forming systems, i. e. in astrophysical objects where the process of dust formation from the gas phase occurs. As will be argued in Sect. 3, the time-dependent process of dust formation introduces new and important dynamical, thermal and radiative feedbacks to the system, which lead to a rather complex behavior of the dust-gas mixture, especially when considered in more than one spatial dimension.

After reviewing some observations of structure formation and self-organization in dust forming objects (Sect. 2), the basic characteristics of the dust formation process are outlined in Sect. 3. Section 4 contains the description of dynamical, thermal and radiative instabilities and respective model calculations for the related structure formation processes. The conclusions are outlined in Sect. 5.

2 Observations

AGB stars: Various high angular resolution observations point to an inhomogeneous distribution of the matter in the outer atmospheres and circumstellar envelopes of AGB stars. Plain evidence is given by direct infrared images (K-band) of the innermost wind region ($\lesssim 20\,R_\star$) of the prominent carbon star IRC+10216 with a spatial resolution better than one stellar radius, obtained by speckle interferometry (Weigelt et al. 1998, Haniff & Buscher 1998, Tuthill et al. 2000). These observations have revealed complex asymmetric dust structures in form of bright knots and outward moving clumps or "bars". Moreover, multi-epoch images allow for important constraints about the mass loss mechanism of these stars as recorded by time-resolved maps of the dust formation and wind acceleration zone.

Further clues to the presence of a cloudy distribution of the dust in AGB star envelopes can be inferred from spectroscopy. Since the ISO-mission, detailed spectra of oxygen-rich AGB and carbon stars are available ranging from the optical to the infrared (20 μm and beyond). The complete energy distribution of these stars is composed of several, apparently independent contributions from the photosphere as well as from the circumstellar dust. Concerning the three carbon stars TX Psc, V 460 Cyg and TT Cyg, Jørgensen et al. (2000) have argued that an inhomogeneous distribution of the dust is neccessary in order to fit both the optical region by direct light from the stellar photosphere *and* the mid IR by thermal emission (~ 500 K) from the circumstellar dust. In contrast, the fit in the optical and near infrared would be destroyed, if the emitting dust was present in a spherical manner which would lead to unavoidable absorption in the near IR, which is not observed.

Arguments for inhomogeneities are furthermore provided by the observations of the patchy SiO maser spots which are formed around $2 - 3\,R_\star$ and possibly map the density and/or temperature distribution in this region. Time series of well-resolved images of the maser emission concerning the oxygen-rich AGB stars TX Cam and IRC+10011 (Diamond & Kemball 1999, Desmurs et al. 2000) show that the individual spots are rather constant in brightness and clearly moving in space, apparently following the hydrodynamical motion of the gas.

On a larger scale, the circumstellar envelopes of AGB stars reveal additional evidence for roughly spherically symmetric structure formation, probably of hydrodynamical nature. Examples for such structures are the multiple shells of IRC+10216 (Mauron & Huggins 2000) or the detached shells of e. g. TT Cyg (Olofsson et al. 2000). Whereas the origin of the former with a typical shell separation of 5"-20" and associated time scale of a few hundred years is not clear at the moment, the detached shells are probably caused by a rather sudden change of the mass loss rate approximately 7 000 yrs ago, which is conform with recent stellar evolutionary models (Schröder et al. 1999). At the interface between the outer, denser and faster wind from an earlier epoch and the inner, thinner and slower wind, shock fronts form which produce the observed overall spherical molecular emission. However, the shocks introduce Rayleigh-Taylor instabilities (Gustafsson et al. 1999) which is identified as possible physical cause of the internal clumpiness of the detached shell as observed with high angular and frequency resolution (Olofsson et al. 2000).

Post-AGB stars: An important fraction of the post-AGB star envelopes shows a non-spherical, often axisymmetric morphology (Lopez 1999), sometimes associated with bipolar outflows. Examples for such shapes are the Egg-Nebulae (Skinner et al. 1997) and the Red Rectangle (Lopez et al. 1997). From the observations, an evolutionary sequence towards a higher level of asymmetry and complexity exists in circumstellar environments, ranging from the early, low mass loss AGB stars via very late type, high mass loss objects at the tip of the AGB (e. g. IRC+10216) towards post-AGB stars and finally planetary nebulae. But it is also possible that the occurrence of inhomogeneities and dispersivity is a rather widespread phenomenon in dusty objects better resolved by observations in case of a larger mass loss rate, simply because of contrast effects (Lopez 1999).

The physical background of the spatial structuring of post-AGB star envelopes is often not very well-understood. Possible candidates are an increase of the magnetic activity and/or the rotation of the central star or the existence of a companion (e. g. Lopez 1999), but the details of the hydrodynamical processes shaping the post-AGB environments are quite uncertain. Two-dimensional radiative transfer models of post-AGB dust shells (Lopez & Perrin 2000) indicate that already small deviations from the spherical symmetry of the spatial dust distribution may cause a clearly non-spherical spectral appearance. First stationary model calculations for a non-spherical mass loss caused by the rotation of the central star have been presented by Dorfi & Höfner (1996), where the radiative transfer, however, has not been solved in a multi-dimensional way.

Planetary nebulae: One of the most remarkable results of the Hubble Space Telescope mission is the discovery of numerous (thousands of) opaque structures in various planetary nebulae (e. g. the Helix and Eskimo nebulae) as well as in star formation regions (e. g. the Orion nebula). These neutral, dense (possibly dusty) regions, named as "cometary knots", "globuls" or "proplyds", are located at the head of *radially aligned linear structures* in the nebula, in particular revealed by high resolution images of emission line ratios (e. g. [OIII]/Hα). The linear structures are possibly connected to the shadows casted from the neutral knots which are optically thick in the Lyman continuum (O'Dell 2000). Attempts to ascribe the long, radially aligned, linear structures to dynamical processes and instabilities (e. g. Dyson et al. 1993) face the difficulty to produce such extended objects with a length of about $1.5 \cdot 10^{16}$cm but a diameter of only 10^{15}cm, which requires fine-tuned parameters. Other works investigate the photoevaporation of the cometary knots (López-Martín 2000) exposed to the UV light from the central star.

Whereas the physical nature of the linear structures is extensively discussed in the literature, the origin of the knots themselves remains mysterious. The density contrast between the knots ($\sim 10^{6}\,\mathrm{cm}^{-3}$, O'Dell & Handron 1996) and the surrounding gas ($\sim 50\,\mathrm{cm}^{-3}$, López-Martín et al. 2000) is remarkably large, indicating a fascinating example of self-organization in space. The large density contrast leads to the astonishing conclusion that a substantial fraction of the mass of the planetary nebulae must be present in form of the neutral knots (López-Martín 2000). Dyson et al. (1989) have proposed that the knots might be relics from the AGB phase of the central star, e. g. from a cloudy distribution of the dust in the former AGB star wind. If this hypotheses is correct, an interesting link would be established between the irregular dust structures observed in very late type AGB stars (e. g. IRC+10216, see above) and the opaque structures in planetary nebulae.

Novae and supernovae: Since long ago, the formation of dust clouds during nova and supernova explosions has been suggested from the observation of their light curves. The observed, rather subtle changes in the optical spectral region instead of a complete "black out" due to efficient dust formation in the ejecta of SN 1987A (Dwek 1988) and the asymmetries of atomic emission lines (blue shifts) at the time of dust formation (Lucy et al. 1989, 1991) indicate a *clumpy distribution of the dust* in the supernova ejecta. Similar observations and conclusions have been obtained for nova explosions (e. g. Chevalier 1981).

These observations are supported by extensive, multi-dimensional numerical simulations of the supernova explosions, where the progenitor star is completely disrupted by the supernova shock wave as a consequence of violent Rayleigh-Taylor instabilities (Hillebrandt 1999, Kifonidis et al. 2000). Furthermore, high resolution Hubble Space Telescope images of the nova T Pyxidis (Shara et al. 1997) clearly show the clumpy or filamentary character of the ejecta of such explosion phenomena.

Warm and hot stars: R Coronae Borealis (RCB) and Wolf-Rayet (WR) stars also show evidence for the formation of fresh dust from the gas phase despite their high effective temperatures in comparison to AGB stars. RCB stars with $T_{\rm eff} \approx 7000\,$K are particularly well-known for their spectacular decline events which occur at unpredictable time intervals. At the onset of a decline, a huge *dust cloud* is formed close to the photosphere which may completely cover the stellar disk. The star is typically obscured within a few weeks (decrease of the visual brightness by up to 9 mag) before it slowly recovers and finally returns to normal brightness on a much longer time scale of typically months or years (Clayton 1996). Comparable observations, though not as concise as for RCB stars, have been obtained for carbon-rich WR stars of late spectral type WC 7 to WC 9 with effective temperatures of about 25 000 K (Crowther 1997, Veen et al. 1998). The spectroscopic and photometric similarities between these these two classes of objects during the declines are remarkable. In both cases, the cloudy character of the dust formation (besides other arguments) is evident from the non-detection of a respective increase of the IR brightness during the visual declines.

The physical processes, which trigger the dust formation events in these hot, hydrogen-poor but carbon-rich objects, are not known precisely. Concerning RCB stars, giant convection cells (Wdowiak 1975) and instabilities deep in the He ionization zone of the stellar atmosphere due to super-Eddington luminosities (Asplund 1998) have been proposed. Woitke et al. (1996b) have shown that shock waves (e. g. caused by the pulsation of the central star) can initiate a two-step cooling of the circumstellar gas (radiative followed by adiabatic cooling after the passage of a shock wave) which may lead to temperatures suitable for carbon nucleation in these hydrogen-poor environments. New high-resolution spectra shortly before and during two decline events of R Coronae Borealis (Kameswara Rao et al. 1999) seem to confirm this link between shock waves and dust formation.

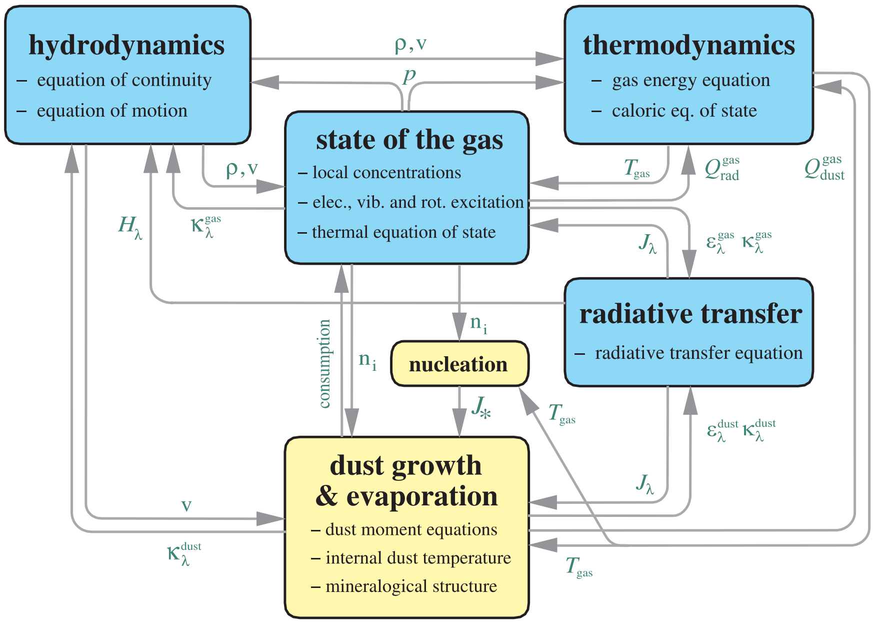

Figure 1: Overview of physical interactions in a dust forming system

3 Dust forming systems

In order to analyze the dynamical behavior and the stability of astrophysical objects where dust formation occurs (dust forming systems), it is worthwhile to realize the various interrelations between the dust formation and the other relevant dynamical, chemical, thermal, and radiative processes (Fig. 1).

The process of dust formation via nucleation and growth is controlled by local physical conditions of the ambient medium: the gas particle densities n_i, the gas temperature $T_{\rm g}$, and the local mean spectral intensity J_λ, which determines the internal dust temperature $T_{\rm d}$ ([1]) and may be directly involved in certain surface reactions like UV sputtering. These physical quantities must be obtained from an adequate solution of hydrodynamics, thermodynamics, radiative transfer and chemistry. However, *the inclusion of dust introduces new and important physical interactions which cause strong feedbacks.* (i) In luminous objects like AGB stars, the dust formation may cause the leading force in the equation of motion by radiative pressure on dust grains. For instance, dust formation is closely related to the mass loss mechanism of cool stars which determines the density structure of the circumstellar envelope. (ii) Dust formation leads to an increase of the overall opacity of the gas-dust

[1]Usually, dust and gas are thermally decoupled in astrophysical objects ($T_{\rm d} \neq Tg$) because of the limited collisional energy exchange which is usually negligible for the dust (but not for the gas!) unless the gas particle density exceeds $\approx 10^{16}\,\rm cm^{-3}$. The assumption of radiative equilibrium for the dust component is therefore justified, also because the radiative relaxation time scales for small grains are typically as short as 0.01 s (Woitke 1999).

mixture by several orders of magnitude. Thereby, the dust plays a decisive role in the radiative transfer with important consequences for the temperature structure. (iii) Dust consumes the condensible elements in the gas phase and may furthermore provide the first catalytic surface sites which can influence the chemical composition of the gas, e. g. by H_2-formation. (iv) The dust component serves as an additional heat bath for the gas, introducing a new source term in the energy equation $Q^{\rm gas}_{\rm dust}$ which accounts for the collisional energy exchange between dust and gas, e. g. thermal accommodation. All these feedbacks are in turn important in order to calculate the local quantities which control the dust formation:

Dust triggers the conditions for its own formation.

Dust forming systems are therefore strongly non-linear coupled systems which contain important dynamic and thermo-kinetic feedbacks. Such system are capable to maintain balance by self-regulation mechanisms, but can also be affected by instabilities. In general, the problem of dust formation in astrophysical objects cannot be treated on the basis of *a priori* known thermodynamical conditions. In contrast, these conditions must be obtained from a simultaneous, consistent solution of the full system sketched in Fig. 1.

4 Instabilities in dust forming systems

Due to the additional feedbacks introduced by the key process of dust formation, the complex physical system sketched in Fig. 1 may host various dynamical, thermal or radiative instabilities not known elsewhere. It is the aim of this paper to identify such instabilities and to discuss the possibility of related self-organization processes in dust forming objects. But before investigating these questions, we outline at first some basic dependencies of the dust formation process on density and temperature.

4.1 Basic characteristics of dust formation

Dust formation from the gas phase is a two-step process of nucleation and growth, which shall be analyzed in the following by means of the moment method developed by Gail & Sedlmayr (1988). The basic idea of this method is to consider moments of the dust size distribution function $f(a)$ where a is the radius of the dust particles, which are assumed to be spherical. The dimensionless dust moments are defined by

$$K_j \;=\; \frac{1}{n_{\langle{\rm H}\rangle}} \int\limits_{a_\ell}^{\infty} f(a) \Big(\frac{a}{a_0}\Big)^j \, da \ . \qquad (1)$$

Often, the exact knowledge of the size distribution function is not at all required, but it is sufficient to calculate certain overall properties like the total surface of the dust component per volume $n_{\langle{\rm H}\rangle} 4\pi a_0^2 K_2$ (necessary to quantify chemical surface reactions, for example) or the total volume fraction of the dust component $n_{\langle H\rangle} 4\pi a_0^3 K_3/3$ (which is proportional to the dust-to-gas ratio ρ_d/ρ_g or the total dust opacity $\kappa_\lambda^{\rm dust}$ in the small particle limit of Mie theory). a_0 is the monomer radius, i. e. the hypothetical radius of one monomer[2] in the solid compound and $n_{\langle H\rangle}$ the total hydrogen particle density.

Only particles larger than a certain minimum size a_ℓ are included. This lower integration boundary is chosen such, that the chemical and radiative properties of the dust particles beyond this size can be calculated by applying solid state physics according to the macroscopic properties of the bulk material. Processes affecting smaller grains (the "clusters") are treated by a net flux in size-space $J(a_\ell)$ through the lower integration boundary. Following time scale arguments (Gail & Sedlmayr 1988), a stationary flow of the particles in size space up to a_ℓ can be assumed, making it possible to identify $J(a_\ell)$ with the nucleation rate $J_\star$ in case of net growth, i. e. the formation rate of seed particles per H-atom. Here, the full details of reaction kinetics among the individual clusters can be considered. Alternatively, one may simplify the problem by applying classical nucleation theory. The formulation has been extended to the case of net evaporation by Gauger et al. (1990).

Assuming that the dust grains are affected by chemical surface reactions only (disregarding coagulation and shattering by grain-grain collisions), the temporal evolution of the dust component is described by the following set of differential equations

$$\frac{dK_0}{dt} = J(a_\ell) \tag{2}$$

$$\frac{dK_j}{dt} = \frac{j}{3\,\tau_{\rm gr}} K_{j-1} + \left(\frac{a_\ell}{a_0}\right)^j J(a_\ell) \qquad (j = 1, 2, 3, ...)\ . \tag{3}$$

d/dt is the Lagrangian time derivative and $\tau_{\rm gr}$ the net growth time scale, i. e. the time required to cover all existing surfaces with one new layer of monomers

$$\tau_{\rm gr}^{-1} = 4\pi a_0^2 \sum_r n_{\mathcal{A}_r}\, v_{\mathcal{A}_r}^{\rm th}\, \alpha_r\, m_r \left(1 - \frac{1}{b_r^{\rm th}\, S^{m_r}}\right) \tag{4}$$

which involves a sum over all contributing surface reactions. All dust grains are hereby assumed to have a uniform temperature $T_{\rm d}$ which, however, may differ from $T_{\rm g}$. For simplicity, we have furthermore assumed that the gas particles are in chemical equilibrium with each other according to the gas temperature $T_{\rm g}$ ([3]). $n_{\mathcal{A}_r}$ is the particle density of the impinging gas particle initiating the reaction r, $v_{\mathcal{A}_r}^{\rm th}$ its thermal velocity, α_r the sticking coefficient and m_r the number of monomers added to the solid particle per reaction. The latter term in Eq. (4) accounts for the reverse reactions by applying Milne relations with respect to the detailed balance. $S = n_{\rm mono} k T_{\rm g}/p_{\rm vap}(T_{\rm g})$ is

[2]The smallest unit building up the solid material, e. g. a carbon atom for graphite or an Al_2O_3-unit for corundum.

[3]This assumption can be relaxed to the more general case of chemical non-equilibrium, see Patzer et al. 1998.

Table 1: Departure coefficients for thermal non-equilibrium $b^{\rm th}$ as function of surface reaction type. $\mathcal{C}_{\rm N}({\rm s})$ means a solid particle composed of N monomers. k_p is the chemical equilibrium constant of the respective molecule.

surface reaction type	$b^{\rm th}(T_{\rm g},T_{\rm d})$
$\mathcal{A}+\mathcal{C}_{\rm N}({\rm s}) \;\rightleftharpoons\; \mathcal{C}_{\rm N+m}({\rm s})$	$\left(\dfrac{p_{\rm vap}(T_{\rm g})}{p_{\rm vap}(T_{\rm d})}\right)^m \dfrac{k_p(\mathcal{A},T_{\rm g})}{k_p(\mathcal{A},T_{\rm d})}\,\sqrt{T_{\rm d}/T_{\rm g}}$
$\mathcal{A}+\mathcal{C}_{\rm N}({\rm s}) \;\rightleftharpoons\; \mathcal{B}+\mathcal{C}_{\rm N+m}({\rm s})$	$\left(\dfrac{p_{\rm vap}(T_{\rm g})}{p_{\rm vap}(T_{\rm d})}\right)^m \dfrac{k_p(\mathcal{A},T_{\rm g})}{k_p(\mathcal{A},T_{\rm d})}\,\dfrac{k_p(\mathcal{B},T_{\rm d})}{k_p(\mathcal{B},T_{\rm g})}$

the supersaturation ratio at gas temperature which expresses the phase non-equilibrium between gas and dust, $n_{\rm mono}$ is the monomer density in the gas phase and $p_{\rm vap}$ the vapor pressure of the considered dust material.

$b^{\rm th}_r$ is the thermal b-factor of the reaction r which accounts for departures from thermal equilibrium between gas and dust. Such deviations are likely to occur in astrophysical objects (see footnote 1). For example, the so-called inverse greenhouse effect (larger dust opacities in the optical than in the infrared spectral region) usually leads to higher dust temperatures as compared to the gas temperature. However, there are also so-called "glassy" dust materials, where this effect may be reverse (Woitke 1999). The thermal b-factors depend on the type of surface reaction (Patzer et al. 1998, see Table 1).

Equation (4) allows for a generalization of the definition of the thermal stability of dust grains by means of $\tau_{\rm gr}^{-1}=0$. The respective sublimation temperature of the dust material can be defined as $T_s(n_{\langle{\rm H}\rangle},T_{\rm g}) = T_{\rm d}\big(\tau_{\rm gr}^{-1}(n_{\langle{\rm H}\rangle},T_{\rm g},T_{\rm d})\!=\!0\big)$. In thermal equilibrium ($T_{\rm d}=T_{\rm g}$), where $b^{\rm th}_r=1$, this matches the usual definition of phase equilibrium $S=1$. However, in thermal non-equilibrium, the criterion is more complicate and depends on the chemical composition of the gas as well as on the considered surface reactions. In application to carbon dust formation for example, where usually $T_{\rm d}>T_{\rm g}$, numerical evaluation of Eq. (4) shows that the growth is dominated by collisions with hydrocarbons, in particular with acetylene, $C_2H_2 + C_N(s) \rightarrow H_2 + C_{N+2}(s)$, whereas the evaporation is not caused by the reverse process, but simply by $C_N(s) \rightarrow C + C_{N-1}(s)$. The stability is hence characterized by a kinetic equilibrium between both reactions, but detailed balance is not achieved as would be the case if $T_{\rm d}=T_{\rm g}$.

Density-dependence: A simple but important case occurs if the conditions for dust formation are constant ($J(a_\ell)=$ const, $\tau_{\rm gr}=$ const). In this case, the moment equations (2) and (3) can be integrated analytically. Neglecting the usually unimportant second term on the r. h. s. of Eq. (3) and considering initial conditions $K_j(t\!=\!0)=0$, the result is

$$K_3(t) \;=\; \frac{J_\star\, t^4}{108\,\tau_{\rm gr}^3}\ , \qquad (5)$$

which states a formula for the temporal increase of the third dust moment during the onset of dust formation. Equation (5) is valid only for short times after the onset of dust formation before any relevant changes of n_i, $T_{\rm g}$, or J_λ occur, e.g. due to hydrodynamical dilution or due to the feedbacks of the dust formation process itself. Therefore, one of the preconditions for deriving Eq. (5) is that the resulting dust quantities remain "small". The density-dependence of the process of dust formation can be easily obtained in this case. The inverse growth time scale (see Eq. 4) is proportional to the gas density. Assuming a density-dependence of the nucleation rate per H-atom of $J_\star \propto {n_{\langle\rm H\rangle}}^{0\ldots1}$, Eq. (5) results in

$$K_3(t) \propto f_{\rm cond}(t) \quad \propto \quad {n_{\langle\rm H\rangle}}^{3\ldots4} \;, \tag{6}$$

independent of the temperatures $T_{\rm g}$ and $T_{\rm d}$. Thus, a gas element which is 10 times denser than a reference element will start to condense out and become optically thick about 10 000 times faster.

Temperature-dependence: The temperature-dependence of the process of dust formation is more complicate. Considering a highly supersaturated gas, $S \gg 1$ in Eq. (4), the growth time scale $\tau_{\rm gr}$ depends only weakly on the temperature, unless the sticking coefficients α_r are strongly temperature-dependent. Consequently (see Eq. 5), the temperature-dependence of the dust formation process mainly results from the nucleation rate $J_\star$.

The calculation of nucleation rates, however, is a matter of debate under astrophysical conditions. Time-dependent calculations of nucleation rates via chemical kinetics require accurate thermodynamical cluster data, the exact knowledge about the chemical pathways leading to larger clusters, and the rates of all involved reaction steps under the prevailing extreme low-pressure conditions. Up to now, such kinetic calculations have only been carried out for polyaromatic hydrocarbon (PAH) cluster, where a large body of experimental data is available from combustion chemistry (e.g. Keller 1987, Frenklach & Feigelson 1989, Cherchneff et al. 1992). But still, the models seem to predict much too small formation yields and difficult questions remain, for example whether or not the clusters are in thermal equilibrium with the gas. Due to these difficulties, former studies have often adopted the principles of classical nucleation theory (for a recent review see e.g. Gail & Sedlmayr 1998).

In one aspect, however, kinetic and classical approaches agree with each other, namely that efficient nucleation is possible only for low temperatures depending on the condensate, typically around $T_n \approx 1000\,$K within a narrow range of a few hundred Kelvin width, which is well below the sublimation temperatures T_s of refractory grains. Therefore, in a large temperature regime between typical nucleation and typical sublimation temperatures $T_n \ldots T_s$, the dust formation process is *marginally stable*, i.e. dust particles would grow if they were present, but cannot form because of the nucleation barrier. Close to T_n, the dust formation process strongly accelerates if the temperature decreases, because of the exponential temperature-dependence of $p_{\rm vap}$ which enters into the supersaturation ratio S and controls the nucleation rate.

The situation is quite different if seed particles are already present in the gas phase, e. g. provided by a different condensate (which can nucleate at even higher temperatures) or in the case when the gas was already once in a much cooler state before. In this case, the further dust formation is mainly controlled by $\tau_{\rm gr}^{-1}$ which shows a strong temperature-dependence with threshold character: positive and weakly dependent at low temperatures, exponentially decreasing close to T_s, and increasingly negative for $T_{\rm d} > T_s$.

In summary, the dust formation process shows very strong, non-linear dependencies on the gas and dust temperatures with *threshold character*. Usually, a lowering of the temperature favors the dust formation. *Memory effects* originate from the nucleation barrier and from the long time scales involved in the chemical processes causing the dust formation, typically months or years at densities $\approx 10^{11}\rm cm^{-3}$, see e. g. Fig. 3 of (Woitke 1999), which can result in a *hysteresis behavior* of the dust-to-gas ratio, for example, if the temperature varies sinusoidally on such a time scale.

4.2 Dust induced shock waves

The first dynamical instability presented here (s. Fig. 2) was already discovered by Fleischer et al. (1991) and has meanwhile also been confirmed by other independent calculations (Höfner et al. 1994). An initial compression of the gas enhances the chemical surface reaction rates responsible for dust growth and hence leads to an acceleration of the dust formation process (see Sect. 4.1). The respective faster increase of the opacity causes a stronger hydrodynamic acceleration of the dust forming zones by radiation pressure on dust grains and frictional coupling between dust and gas. The larger velocities of the dust forming zones lead to a further compression of the medium, which is situated behind these zones. Thus, an overall positive feedback is given (Fig. 2), i. e. an self-amplifying control loop is established, which amplifies initial perturbations in the system. The latter, non-local effect by compression causes a wave-like behavior of these disturbances, propagating outward.

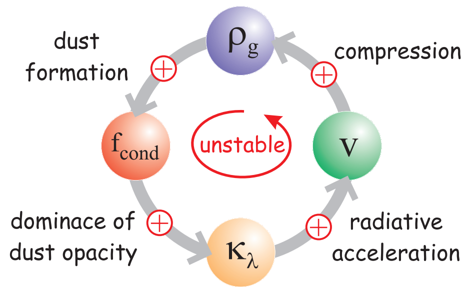

Figure 2: Dust induced shock waves as dynamical instability. Positive feedbacks are marked by ⊕, negative feedbacks by ⊖. $\rho_{\rm g}$ = gas density, $f_{\rm cond}$ = degree of condensation, κ_λ = spectral extinction coefficient, v = hydrodynamical velocity.

The formation of dust induced shock waves has been studied in the framework of time-dependent, spherically symmetric model calculations, which include hydrodynamics, chemical equilibrium, modified classical nucleation theory, a time-dependent treatment of dust growth and evaporation, and grey radiative transfer (Fleischer et al. 1992, Helling et al. 2000a, Winters et al. 2000). The considered system of differential equations contains important thermo-kinetic feedbacks via the extremely temperature-dependent process of nucleation (see Sect. 4.1) and is globally coupled by the radiative transfer.

The results of these model calculations indicate that the cool outflows of AGB stars are generally *not* expected to contain a homogeneous dust distribution (Fig. 3). The pulsation of the central star[4] creates acoustic waves, which steepen into shock waves during the passage through the atmosphere along its large density gradient. These shock waves penetrate deeply into the circumstellar envelope, accelerating the gas outward, and cause a time-dependent levitation of the outer atmosphere, i. e. a considerable increase of the densities as compared to static or stationary models. Thereby, the dust formation is substantially favored during certain limited time intervals related to the passage of the pulsational shock waves. Consequently, the dust forms in a discontinuous way, resulting in a layered dust structure. Amplified by the mechanism described above, the coupled phenomenon of dust formation and shock wave propagates outward. A characteristic feature of the dust induced shock waves is the formation of local density inversions in the post-shock regions, indicating the strong radiative acceleration of the forming dust behind the shock waves. Leaving aside non-spherical effects, these dust induced shock waves provide the most prominent spatio-temporal structure formation phenomenon in the circumstellar envelopes of AGB stars. More details about these models have been presented by Helling et al. (2000b) concerning Large Magellanic Cloud models, Jeong et al. (2000) for oxygen-rich AGB stars, and Schirrmacher et al. (2000) for detailed non-LTE cooling functions.

The time-dependent formation, radiative acceleration and radial dilution of the dust shells introduces a new characteristic internal time scale $\tau_{\rm dust}$ to dust forming systems, which may interfere with the pulsational period P of the star. Consequently, the dynamical behavior of dust forming circumstellar envelopes is similar to a periodically driven oscillator characterized by its eigenfrequency. In the numerical models, the formation of dust shells close to the star occurs in fact in mono-periodic, multi-periodic or even chaotic time intervals, depending on the relation between $\tau_{\rm dust}$ and P (Fleischer et al. 1995). A mathematical analysis of the stability and dynamical behavior of such dust forming systems has been presented by Meier et al. (2000), applying standard techniques from the theory of dynamical systems to a simplified model of non-linearly coupled, spherically symmetric, dust forming Lagrangian zones. The results indicate that an unstable situation occurs for certain values of the eigenfrequency of the innermost shell divided by the pulsational frequency, where the system can stabilize itself by the ejection of the outermost shell.

[4]Simulated by a sinusoidal motion of the innermost grid point of the model ("piston").

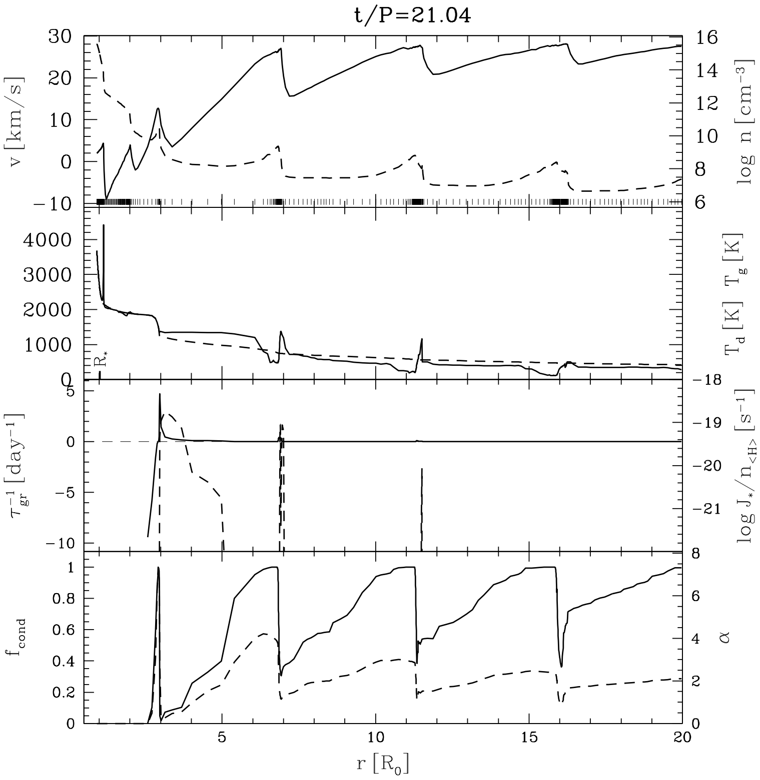

Figure 3: Dust induced shock waves in the circumstellar envelope of a C-star according to a spherically symmetric model calculation. Note the common occurrence of dust, enhanced densities and enhanced velocities. v = hydrodynamical velocity, n = gas particle density (dotted), $T_{\rm g}$ = gas temperature, $T_{\rm d}$ = dust temperature (dotted), $\tau_{\rm gr}^{-1}$ = inverse dust growth time scale in units of atomic layers/day, J_* = nucleation rate per hydrogen nucleus (dotted), $f_{\rm cond}$ = degree of condensation of carbon, α = ratio of radiative acceleration to gravitational deceleration (dotted).

4.3 Thermal bifurcations

Usually in dust forming objects, the energy balance of the gas is dominated by radiative heating and cooling rates, since other energy transfer processes like heat conduction or convection are insignificant under the prevailing low densities and intense radiation fields. Consequently, the corresponding equilibrium state is characterized by an equality of radiative gains and losses. However, as was already shown by Ayres (1981), the condition of radiative equilibrium (RE) is not always unique, but allows for several solutions with different temperatures and compositions ("thermal bifurcations").

This thermal multi-stability is caused by the temperature-dependent chemical composition of the gas. The concentrations of the electrons, ions, atoms and molecules trigger the various radiative heating and cooling rates, which altogether yield the total net radiative cooling function $Q_{\rm rad}$, which

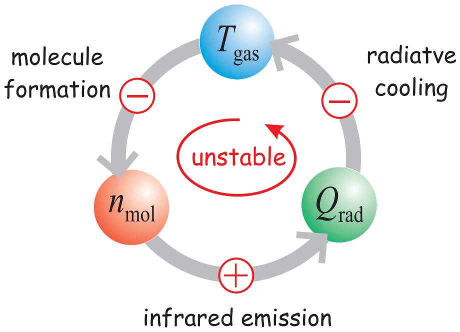

Figure 4: Thermal instability in partially molecular gases. $T_{\rm gas}=$ gas temperature, $n_{\rm mol}=$ molecular concentrations, $Q_{\rm rad}=$ net radiative cooling rate.

vanishes in RE. Since the concentrations themselves depend non-linearly on the gas temperature, a control loop is established (see Fig. 4), which allows for different stable and unstable solutions. In particular, at sufficiently low temperatures, molecules will form which strongly contribute to the radiative cooling of the gas because of their numerous permitted ro-vibrational transitions in the infrared and microwave spectral region, thus enforcing a further cooling of the gas. Consequently, two major types of radiative equilibrium solutions exist: one being molecule-rich at low temperatures and the other one being molecule-poor at high temperatures.

The role of the non-uniqueness of the condition of radiative equilibrium for the structure and the dynamics in stellar atmospheres and circumstellar envelopes has only been little investigated in detail, especially concerning the outer atmosphere of the sun (Kneer 1983, Muchmore 1986). An important link to the onset of dust formation in cool giants has been proposed by Cuntz & Muchmore (1994). By means of the thermal bifurcations, the low gas temperatures necessary for the nucleation process can be reached already close to the star, possibly triggered by occasional hydrodynamical expansion which causes additional adiabatic cooling, e. g. during the re-expansion phase after the passage of shock waves.

In order to investigate the radiative energy balance of circumstellar gases, detailed model calculations of the relevant radiative heating and cooling rates are required. Since the densities in dust forming systems are often as low as $10^{10}\rm cm^{-3}$, local thermodynamical equilibrium (LTE) is usually not maintained and the investigations have to account for the important non-LTE effects. The following model calculations are based on the method described by Woitke et al. (1996a). The gas is assumed to be optically thin in the continuum. Optical depth effects in spectral lines are accounted for in an approximate way. The non-LTE ionization balance and level populations are calculated in statistical equilibrium, and the molecular concentrations in chemical equilibrium. The radiative heating/cooling rates are determined from the various free-free (f-f) and bound-free (b-f) transitions, atomic lines and molecular ro-vibrational transitions. The model atoms include several thousand per-

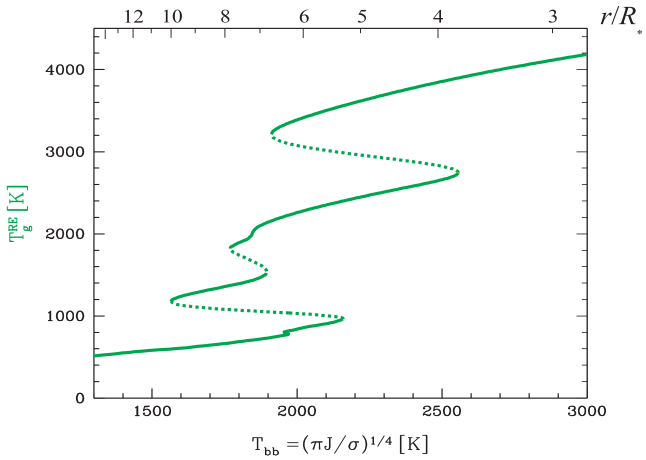

Figure 5: Thermal bifurcations in the outer atmosphere of R Coronae Borealis. $T_{\rm g}^{\rm RE}$ are the calculated radiative equilibrium gas temperatures, where $Q_{\rm rad} = 0$. $r/R_\star$ is the radial distance in units of the stellar radius. The dotted lines indicate the unstable branches of the solutions. $T_{\rm bb}$ is the black body temperature in the considered background radiation field $J_\lambda^{\rm cont}(r)$ (see text). The gas density is fixed in this plot: $\rho_{\rm g} = 10^{-14}\,{\rm g/cm^3}$.

mitted and forbidden lines, and b-f transitions from the ground states and the excited levels of 13 elements in the neutral and first ionization state (see Woitke & Sedlmayr 1999). 23 molecules including CO, SiO, CS, SiS, H_2, H_2O, C_2H_2, HCN and CO_2 are taken into account with 100–10000 levels and 1000–30000 lines each. The non-LTE treatment of the molecules is restricted to the calculation of individual rotational and vibrational excitation temperatures, including overtone transitions, combination bands, quadrupole transitions (in case of H_2) and the important ro-vibrational pumping effect.

By means of such model calculations, it has been shown in (Woitke & Sedlmayr 1998) that the background radiation field of C-stars is usually not intense enough in order to maintain a high-temperature, mainly atomic state in RE close to the star. Instead, the gas is generally characterized by the cool, molecular solution of RE. Similar conclusions have been obtained for oxygen-rich AGB stars (Woitke & Schirrmacher 1999), where some minor bifurcations may be present at low temperatures due to the formation of H_2O.

The results are different for the outer atmospheres of R Coronae Borealis stars (see Sect. 2), where the thermal bifurcations may be of crucial importance for the onset of the spectacular decline events. In the radiation field of these stars both the atomic, and the molecular solutions can exist. For the model calculation depicted in Fig 5, the continuous radiation field $J_\lambda^{\rm cont}(r)$ is assumed to be given by $J_\lambda^{\rm cont}(r)/J^{\rm cont}(r) = F_\lambda/F$, where F_λ is the stellar flux provided by a hydrostatic model calculation for the hydrogen-deficient prototype star R Coronae Borealis (Asplund et al. 1997 with $T_{\rm eff} = 7000$ K and $\log(g) = 0.5$) and $J^{\rm cont}(r) = \sigma T_{\rm eff}^4/2\pi\big(1 - \sqrt{1-(R_\star/r)^2}\big)$. Up to five simultaneous stable RE-solutions are found. Typically, there is one stable, mainly atomic branch ($T_\mathrm{g}^\mathrm{RE} > 3000\,\mathrm{K}$), one branch where atomic heating is balanced by molecular cooling in a stable way ($2000\,\mathrm{K} < T_\mathrm{g}^\mathrm{RE} < 3000\,\mathrm{K}$), and one or more stable low-temperature branches dominated by molecular heating and cooling alone. In between, unstable branches with ($\partial Q_\mathrm{rad}/\partial T_\mathrm{g} < 0$) appear.

Thus, at a given radial distance, the cool molecular and the hot atomic states in RE may principally coexist side by side, possibly leading to an inhomogeneous formation of dust. Close to the bifurcation points, slight changes of the background radiation field (e.g. due to pulsations) may result in considerable, sudden temperature changes, possibly related to the sudden onset of dust formation during the decline events observed in these stars.

4.4 Radiative instability of dust formation

One of the principal results of the dynamical modeling of dust forming systems reviewed in Sect. 4.2 is the strong non-local feedback of the dust formation on the temperature structure of the medium as a result of radiative transfer effects. In particular, the so-called *backwarming effect* has important consequences, i.e. the increase of the radiation field due to scattering and thermal re-emission from the already condensed zones. In spherical symmetry, this effect leads to an *increase* of the temperatures inside of a dust forming shell which temporarily inhibits further nucleation and hence further dust production. Close inspection of Fig. 3 shows, for example, that a dust shell may already start to evaporate "from the inside" during its formation. If we now allow for deviations from spherical symmetry, the radiative transfer effects are more pronounced and even more complex.

> *What are the important radiative transfer effects and how do they influence the dust formation in case of a non-spherical distribution?*

This question lead us to the next kind of instability as sketched in Fig. 6. In radiative equilibrium, a decrease of the mean spectral intensities J_λ is accom-

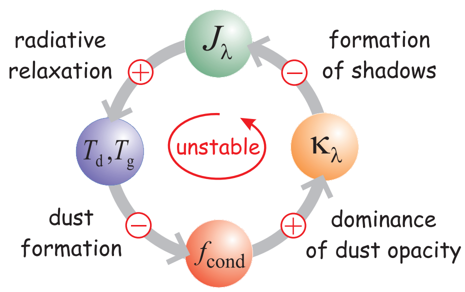

Figure 6: Radiative instability of dust formation. Note the non-local character of the interaction between extinction and mean intensity. J_λ = mean spectral intensity, T_g = gas temperature, T_d = dust temperature, f_cond = degree of condensation, κ_λ = spectral extinction coefficient.

panied by a respective decrease of the gas and dust temperatures $T_{\rm g}, T_{\rm d}$ ($\oplus$). Thereby, the formation of dust is generally favored (see Sect. 4.1), resulting in an acceleration of the dust formation process ($\ominus$). A larger degree of condensation $f_{\rm cond}$ causes a larger local opacity κ_λ of the dust-gas mixture ($\oplus$) which influences the radiation field in a non-local way. In spherical symmetry and radiative equilibrium, $\delta J/\delta\kappa > 0$ is valid in the grey case as evident from the monotonically increasing $J(\tau)$-relation in grey stellar atmospheres (e.g. Mihalas 1978, p. 55). Consequently, the sign of the overall feedback in the control loop depicted in Fig. 6 is usually negative in spherical symmetry ($\oplus \cdot \ominus \cdot \oplus \cdot \oplus = \ominus$), i.e. the control loop is stable against perturbations.

However, if we abandon the assumption of spherical symmetry, the latter interaction may have the opposite effect (Woitke et al. 2000), because a *local* enhancement of the opacity can result in the formation of a *shadow*. Inside this shadow, the mean intensities J_λ decrease ($\ominus$), leading to an overall positive feedback in the control loop ($\oplus \cdot \ominus \cdot \oplus \cdot \ominus = \oplus$). Thus, the dust forming system can be self-amplifying, i.e. unstable against perturbations of various kinds due to multi-dimensional radiative transfer effects.

In order to simulate this radiative instability and to study related structure formation processes in C-star star envelopes, we have developed an axisymmetric numerical model which combines equilibrium chemistry, modified classical nucleation theory (Gail et al. 1984) and time-dependent dust growth, evaporation and element depletion (Gail & Sedlmayr 1988, Gauger et al. 1990, see Eqs. 2 and 3) with frequency-dependent radiative transfer. The absorption and angle-dependent scattering coefficients of the forming dust grains are calculated by applying Mie-theory (Wiscombe 1980) to spherical solid particles with the optical data of amorphous carbon (Rouleau & Martin 1991) according to the resultant dust size distribution function. The transfer part has been kindly provided by B. Lopez (Lopez et al. 1995) and solves the axisymmetric, explicitly time-independent radiative transfer problem in the circumstellar dust shell by means of a Monte-Carlo method, assuming the dust grains to be in radiative equilibrium and to have a size-independent temperature $T_{\rm d}$. The inner boundary is prescribed by a black body of effective temperature $T_{\rm eff}$. Outer irradiation is neglected. The gas is assumed to be optically thin, grey, and in radiative equilibrium, resulting in $T_{\rm g} \equiv T_{\rm bb}$, where $T_{\rm bb} = (\pi J/\sigma)^{1/4}$ is the black body temperature. Both temperature structures $T_{\rm d}(r, \phi, t)$ and $T_{\rm d}(r, \phi, t)$ are hence a direct result of the radiative transfer part, where r is the radius and ϕ the azimuth angle measured from the equatorial plane.

The code has been parallelized and adapted to the given problem in several ways. By implementing a new method for temperature determination according to Lucy (1999), the intrinsic Monte-Carlo noise in the temperature determination has been reduced to less than 0.5 K when using about 40 000 000 photon packages, even in the optically thin cells. The model uses 35 frequency grid points ($\lambda_k = 0.1 \ldots 250\,\mu$m) and 35×25 spatial grid points ($r_i = 3.0 \ldots 5.5 R_\star$ and $\phi_j = -90° \ldots 90°$). The calculations have been performed on a Cray T3E parallel computer, using typically 100 processors.

There are no velocity fields considered in this model. The density dis-

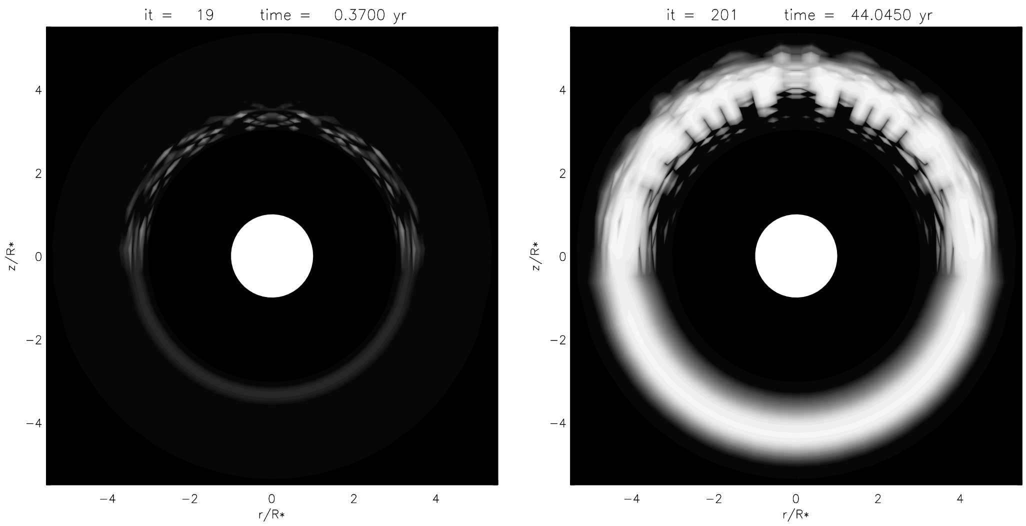

Figure 7: Self-organization and spatio-temporal structure formation – triggered by radiative instabilities – during the formation of a dust shell in the circumstellar envelope of a C-star. The figures represent the logarithmic degree of condensation of carbon $\log(f_{\rm cond}) = -2.5\ldots0$ as function of space at an early (l.h.s.) and a late phase (r.h.s.) as indicated on top. Black means negligible condensation, white complete condensation. In the upper half of the model ($z>0$), a slightly inhomogeneous spatial density distribution is assumed (see text), whereas for comparison, the density distribution is spherically symmetric in the lower half of the model. Parameters: $T_{\rm eff} = 3600\,$K, $R_\star = 10^{13}\,$cm and C/O$\,=2$.

tribution is assumed to be constant in time and given by $n_{\langle{\rm H}\rangle}(r,\phi) \propto \exp\big(-r/H + {\rm z}(\phi)\big)$, where $H = 0.25R_\star$ is a scale height and ${\rm z}(\phi)$ is a random number with Gaussian distribution. The standard deviation of z is chosen in such a way that the density varies randomly by 0.15 dex in the upper half of the model, whereas it is chosen to be zero in the lower half, yielding a spherical density distribution there. The initial state of the circumstellar envelope at $t=0$ is chosen to be dust-free. Thereby, the quasi-static formation of dust in an inhomogeneous C-star environment is considered.

The results of this model calculation[5] are depicted in Fig. 7. The denser regions close to the star begin to condense first, because of the strong density-dependence of the process of dust formation (Sect. 4.1). Consequently, the spatial dust distribution at first resembles the inhomogeneous density distribution in the circumstellar shell (l.h.s. of Fig. 7) with a cutoff at the inner edge as a consequence of the temperature being too high for nucleation close to the star. The process of dust formation continues for a while in this way, until the first zones become optically thick. Each already optically thick zone casts a shadow into the circumstellar envelope wherein the temperatures decrease by several 100 K which improves the conditions for further dust formation. At

[5]See also mpeg-movie at `http://export.physik.tu-berlin.de/~woitke/sfb555.html`

the same time, scattering and re-emission from the already condensed zones intensifies the radiation field in the regions which are situated between the optically thick zones. The stellar flux now escapes preferentially through these segments which are still optically thin, thereby heating them up and worsening the conditions for further dust formation therein. These two contrary effects amplify the initial spatial contrast of the degree of condensation introduced by an inhomogeneous density distribution.

As time passes, the optical depths in the circumstellar environment generally increase and may exceed unity. Consequently, the inner part of the circumstellar envelope heats up considerably and the forming dust "shell" starts to evaporate from the inside, like in the one-dimensional hydrodynamical models shown in Sect. 4.2. Thereby, a stable self-regulating mechanism takes control. The evaporation of the dust shell continues until the back-warming effect is reduced accordingly. Thus, the temperatures at the inner edge of the dust shell finally reach about the sublimation temperature of the dust grain material as defined in Sect. 4.1.

However, the sublimation temperature depends on the density. Denser regions are more resistant against evaporation, because the partial pressures are higher and hence the supersaturation ratios are larger. Consequently, the dense parts of the inner edge of the dust shell remain, whereas the slightly thinner parts evaporate completely (r.h.s. of Fig. 7). In the shadowed regions behind the remaining "clouds", the conditions for the subsequent formation and the survival (i. e. the thermal stability) of the dust are improved due to shielding effect. Thus, *radially aligned, cool, linear dust structures* finally result, oriented according to the preferred direction of the radiation field and surrounded by warmer almost dust-free regions.

5 Conclusions

According to the strong influence of density and temperature on the dust formation process, small perturbations in astrophysical objects (e. g. density inhomogeneities, turbulent velocity fields (see Helling et al. 2000c), temperature fluctuations) will naturally result in large spatial variations of the forming dust component. Moreover, considering partially molecular gases exposed to a distant source of radiation, the non-uniqueness of the condition of radiative equilibrium *(thermal bifurcations)* allows for a spatial coexistence of warm and cool regions, both in radiative equilibrium and in pressure equilibrium with the surroundings. Only in the cool, molecule-rich phase, the temperature is sufficiently low in order to initiate the dust formation process via nucleation. Hence, thermal bifurcations are expected to be involved in the development of an initially irregular dust distribution, especially in hot star environments like RCB and WR stars.

During the dust formation process, strong additional *thermal, dynamical and radiative feedbacks* are present in the physical system, which take control either by stabilizing the system (self-regulation) or by destabilizing the system due to instabilities, depending on the circumstances. Such instabilities amplify the spatial contrasts already present in the forming dust component, possibly initiating large-scale *structure formation* and *self-organization processes* as observed in many astrophysical objects.

One example for such instabilities originates from the strong radiative pressure on dust grains in luminous objects, which causes an unstable dynamical behavior of the dust-gas mixture during the dust formation process: *dust induced shock waves*. This instability results in the formation of dust shells rather than a uniform dust distribution in time-dependent, spherical model calculations of the circumstellar envelopes of AGB stars. However, the underlying physical mechanism is more general (not restricted to spherical symmetry) and is expected to cause always a spatial structuring of dust forming gases in the radial direction.

A different type of instability occurs, when time-dependent dust formation and multi-dimensional radiative transfer are combined. In the models, this *radiative instability of dust formation* leads to a tangential structuring of a circumstellar dust shell. Already condensed zones cast a shadow into the circumstellar envelope, which improves the conditions for subsequent dust formation in the cooler regions shielded from the radiation field. A tangential perturbation of the dust shell is hence amplified, resulting in the development of *linear, radially aligned dust structures*, oriented according to the preferred direction of the radiation field and surrounded by warmer, almost dust-free regions. These structures are similar to certain structures observed in planetary nebulae, suggesting a hypothetical link between the formation of dust clouds in the final AGB phase (e. g. IRC+10216) and the cometary knots in planetary nebulae.

Many open question remain, however, when considering possible interrelations between the hydrodynamical and the radiative transfer effects in circumstellar dust shells. According to a time scale discussion (Woitke et al. 2000), an expanding wind can provide a slowly changing hydrodynamical frame, wherein the faster radiative, chemical and dust formation processes have sufficient time to interact with each other and to amplify internal perturbations by unstable control loops. However, more detailed investigations are required here, which must combine time-dependent, hydrodynamical models of the dust formation process with radiative transfer calculations in more than one spatial dimension.

One possible scenario for the dust formation in circumstellar environments is the following: Dust clouds, formed from inhomogeneities and enlarged by radiative instabilities, are accelerated by radiation pressure in the radial direction, while the illuminated, warmer and less dust containing regions between them stay behind or even fall back. The gas behind such a dust cloud (in radial direction) is shielded from the stellar radiation field, i. e. cooler, and will be compressed because of the dust cloud approaching it. Both effects improve the conditions for subsequent dust formation behind already existing dust clouds, possibly resulting in an inhomogeneous, non-spherical mass loss, thereby breaking the spherical symmetry of the object spontaneously.

Acknowledgments: The author is grateful to Dr. Bruno Lopez for his collaboration and introduction to Monte-Carlo radiative transfer and to Gilles Niccolini for fruitful discussions and cowork concerning the numerical changes and improvements of the transfer code. I want to express my special thanks to Dr. Christiane Helling for her valuable comments on the manuscript and to Dr. Martin Asplund who provided the theoretical spectrum of R Coronae Borealis. This work has been supported by the DFG, Sonderforschungsbereich 555, *Komplexe Nichtlineare Prozesse*, Teilprojekt A3, and by the DAAD in the PROCOPE program under grant D/9822849 and 99001. The numerical computations were performed on the T3E parallel computer at the Konrad-Zuse-Zentrum für Informationstechnik Berlin, project bvpt17.

References

Asplund M., 1998, A&A 330, 641

Asplund M., Gustafsson B., Kiselman D., Eriksson K., 1997, A&A 318, 521

Ayres T. R., 1981, ApJ 244, 1064

Biermann P., Kippenhahn R., Tscharnuter W., Yorke H., 1972, A&A 19, 113

Cherchneff I., Barker J. R., Tielens A. G. G. M., 1992, ApJ 401, 269

Chevalier R. A., 1981, ApJ 251, 259

Clayton G. C., 1996, PASP 108, 225

Crowther P. A., 1997, MNRAS 290, L59

Cuntz M., Muchmore D. O., 1994, ApJ 433, 303

Desmurs J., Bujarrabal V., Colomer F., Alcolea J., 2000, A&A 360, 189

Diamond P. J., Kemball A. J., 1999, In Le Bertre T. et al., *IAU Symp. 191: AGB stars*, p. 195, ASP

Dorfi E., Höfner S., 1996, A&A 313, 605

Dwek E., 1988, ApJ 329, 814

Dyson J. E., Hartquist T. W., Pettini M., Smith L. J., 1989, MNRAS 241, 625

Dyson J. E., Hartquist T. W., Biro S., 1993, MNRAS 261, 430

Fleischer A. J., Gauger A., Sedlmayr E., 1991, A&A 242, L1

Fleischer A. J., Gauger A., Sedlmayr E., 1992, A&A 266, 321

Fleischer A. J., Gauger A., Sedlmayr E., 1995, A&A 297, 543

Frenklach M., Feigelson E. D., 1989, ApJ 341, 372

Gail H.-P., Sedlmayr E., 1988, A&A 206, 153

Gail H.-P., Sedlmayr E., 1998, In Hartquist T., Williams D., *The Molecular Astrophysics of Stars and Galaxies*, p. 285, Oxford Science Pub.

Gail H.-P., Keller R., Sedlmayr E., 1984, A&A 133, 320

Gauger A., Gail H.-P., Sedlmayr E., 1990, A&A 235, 345

Gustafsson B., Myasnikov A. V., Eriksson K., 1999, In Hron J., Höfner S., *Abstracts of the 2nd Austrian ISO Workshop: Atmospheres of M, S and C Giants*,

p. 99, Vienna

Haniff C. A., Buscher D. F., 1998, A&A 334, L5

Helling Ch., Winters J. M., Sedlmayr E., 2000a, A&A 358, 651

Helling Ch., Arndt T. U., Sedlmayr E., 2000b, AG Abstr. Ser. 17, 55

Helling Ch., Lüttke M., Sedlmayr E., Oevermann M., Klein R., 2000c, AG Abstr. Ser. 17, 8

Hillebrandt W., 1999, In Diehl R., Hartmann D., *Astronomy with Radioactivities*, MPE Report 274, p. 117, Schloss Ringberg

Höfner S., Feuchtinger M. U., Dorfi E. A., 1995, A&A 297, 815

Inogamov N. A., 1999, Astrophysics and Space Physics Reviews, Vol. 10, Russian Academy of Sciences, Moscow

Jeong K. S., Sedlmayr E., Winters J. M., 2000, AG Abstr. Ser. 17, 30

Jørgensen U. G., Hron J., Loidl R., 2000, A&A 356, 253

Kameswara Rao N., Lambert D. L., Adams M. T., Doss D. R., Gonzalez G. et al., 1999, MNRAS 310, 717

Keller R., 1987, In Léger A. et al., *Polycyclic Aromatic Hydrocarbons and Astrophysics*, p. 387, Reidel Publ. Comp.

Kifonidis K., Plewa T., Janka H.-T., Müller E., 2000, ApJL 531, L123

Kneer F., 1983, ApJ 128, 311

Lopez B., 1999, In Le Bertre T. et al., *IAU Symp. 191: AGB stars*, p. 409, ASP

Lopez B., Perrin J.-M., 2000, A&A 354, 657

Lopez B., Mékarnia D., Lefèvre J., 1995, A&A 296, 752

Lopez B., Tessier E., Cruzalèbes P., Lefèvre J., Le Bertre T., 1997, A&A 322, 868

López-Martín L., Raga A., Mellema G., Henney W., Cantó J., 2000, accepted by ApJ

Lucy L. B., 1999, A&A 344, 282

Lucy L. B., Danziger I. J., Goiffes C., Bouchet P., 1989, In Tenorio-Tagle G. et al., *Structure and Dynamics of the Interstellar Medium*, p. 164

Lucy L. B., Danziger I. J., Goiffes C., Bouchet P., 1991, In Woosley S. E., *Supernovae*, p. 82, Springer Verlag

MacDonald J., Mullan D., 1997, ApJ 481, 963

Mauron N., Huggins P. J., 2000, A&A 359, 707

Meier S., Patzer A., Lüttke M., Woitke P., Sedlmayr E., 2000, AG Abstr. Ser. 17, 56

Mihalas D., 1978, *Stellar Atmospheres*, W. H. Freeman and Company, 2^{nd} edition

Muchmore D., 1986, A&A 155, 172

O'Dell C. R., 2000, AJ 119, 2311

O'Dell C. R., Handron K. D., 1996, AJ 111, 1630

Olofsson H., Bergman P., Lucas R., Eriksson K., Gustafsson B. et al., 2000, A&A 353, 583

Patzer A. B. C., Gauger A., Sedlmayr E., 1998, A&A 337, 847

Rouleau F., Martin P. G., 1991 ApJ 377, 526

Schirrmacher V., Woitke P., Sedlmayr E., 2000, AG Abstr. Ser. 17, 64

Schröder K.-P., Winters J. M., Sedlmayr E., 1999, A&A 349, 898–906

Shara M. M., Zurek D. R., Williams R. E., Prialnik D., Gilmozzi R. et al., 1997, AJ 114, 258

Skinner C. J., Meixner M., Barlow M. J., Collison A. J., Justtanont K. et al., 1997, A&A 328, 290

Spiegel E. A., 1957, ApJ 126, 202

Trujillo Bueno J., Kneer F., 1990, A&A 232, 135

Tuthill P., Monnier J., Danchi W., Lopez B., 2000, ApJ 543, 284

Veen P. M., van Genderen A. M., van der Hucht K. A., Li A., Sterken C., Dominik C., 1998, A&A 329, 199

Wdowiak T. J., 1975, ApJ 198, L139

Weigelt G., Balega Y., Blöcker T., Fleischer A. J., Osterbart R., Winters J. M., 1998, A&A 333, L51

Winters J. M., Le Bertre T., Jeong K. S., Helling Ch., Sedlmayr E., 2000, A&A 361, 641

Wiscombe W. J., 1980, Applied Optics 19, 1505

Woitke P., Sedlmayr E., Lopez B., 2000, A&A 358, 665

Woitke P., 1999, In Diehl R., Hartmann D., *Astronomy with Radioactivities*, MPE Report 274, p. 163, Schloss Ringberg

Woitke P., Schirrmacher V., 1999, In Hron J., Höfner S., *Abstracts of the 2nd Austrian ISO Workshop: Atmospheres of M, S and C Giants*, p. 23, Vienna

Woitke P., Sedlmayr E., 1999, A&A 347, 617

Woitke P., Sedlmayr E., 1999, In Le Bertre T. et al., *IAU Symp. 191: AGB stars*, Poster P3–17, ADS

Woitke P., Krüger D., Sedlmayr E., 1996a, A&A 311, 927

Woitke P., Goeres A., Sedlmayr E., 1996b, A&A 313, 217